Adhesion and Wrapping in Colloid−Vesicle Complexes

Markus Deserno* and William M. Gelbart

Department of Chemistry and Biochemistry, University of California, Los Angeles, 405 Hilgard Avenue, Los Angeles, California 90095-1569

Received: October 17, 2001; In Final Form: February 13, 2002

We present a simple theoretical model for adsorption of colloidal particles onto vesicles. The contact energy of adhesion is balanced by the tension and curvature energies of the vesicle membrane under the constraint of fixed volume, with the geometry of the complex determined by a variational calculation. Physical observables, such as the degree of penetration or the membrane tension, are investigated as functions of colloidal size and adhesion, tension, and bending energies. We find various new (and discontinuous) transitions in the geometry of the complex compared to those from a description that neglects the curvature contribution. Particular emphasis is put on the transition from the partly to the fully wrapped state and on unbinding of the complex at weak adhesion energy or small colloidal size. The above model can be thought of as a phenomenological theory of the initial steps involved in biological endocytosis and aims toward an improved physical understanding of this process.

1. Introduction

The control of transport through cell membranes is fundamental to biological function. The sizes of particles entering and leaving the cell commonly range over several orders of magnitude, from angstroms to microns, and the nature of these particles varies from small atomic ions (notably Na^+ and Ca^{2+}) to large viral particles. For the transport of small atomic ions, membrane proteins of various kinds have been shown to act as channels or transporters, locally facilitating the passage of the solute into the cytoplasm.[1] A great deal has been deduced about the structure and dynamics of these systems. In the case of viruses, on the other hand, the entry and exit processes are entirely different; here, the membrane needs to *envelop* the particle (typically tens to hundreds of nanometers in size[2]) and thereby *deform* on a scale that is large compared to its thickness (just a few nanometers).[3] This latter process—the passage of a particle into (and out of) the cell via "invagination" and subsequent "fission" of the membrane (see Figure 1)—is known as endocytosis (and exocytosis)[1,4] and is rather poorly understood. Impressive molecular-level scenarios have been worked out for receptor-mediated binding of viral particles, for example,[1,4,5] but few experiments or theories have addressed the underlying *physics* of the adhesion and wrapping of particles that start on one side and end up on the other side of the membrane. While most often a cellular mechanism of protein (e.g., clathrin) aggregation induces the membrane deformation, there are important examples in which the adhesion energy between the membrane and the cargo itself is believed to be the driving force for wrapping—an example is the maturation of type-D retroviruses, which involves the budding of preassembled viral core particles at the plasma membrane.[6,7]

In the present work, we treat the interaction of a unilamellar vesicle (model membrane) with a small colloidal particle (model viral capsid), taking into account the adhesion between the two and the stretching and bending energy of the membrane. In various levels of approximation, we determine the equilibrium (minimum-energy) configuration of the complex, which consists of the particle wrapped (enveloped) by the membrane, or both. We establish sets of conditions for which the particle is unbound, partially wrapped, and fully enveloped. These conditions correspond to various combinations of the physical properties of the system, for example, the ratio of adhesion and membrane stretching energies, the ratio of particle and vesicle size, and the bending energy of the membrane. Because full envelopment is a necessary condition for endo/exocytosis, we argue that these various physical quantities provide a basis for understanding the necessary conditions for passage of colloidal particles through cell membranes.

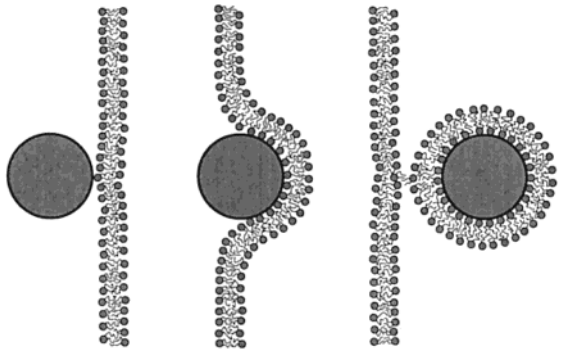

Figure 1. Schematic representation of the process of endocytosis. A particle crosses a barrier imposed by a fluid lipid membrane via a wrapping and subsequent fission process.

In section 2, we first consider the adhesion problem from the point of view of energetics. From there, we outline in section 3 the possible scenarios for adhesion and wrapping of a colloidal particle by a unilamellar vesicle that occur as a balance between adhesion and stretching energy, as suggested by a recent experimental and theoretical analysis.[8] These authors argue that the curvature elasticity of the membrane can be neglected because of the sufficiently large diameter of the colloidal particles and vesicles under study. To be able to describe adhesion for smaller systems, we include explicitly in section 4 the bending energy of the bilayer and formulate a simple

* To whom correspondence should be addressed. E-mail: markus@chem.ucla.edu.

10.1021/jp0138476 CCC: $22.00
Published on Web 04/27/2002

variational approach for treating the equilibrium shape of the membrane in its wrapping complex with the colloid. Complete envelopment of the particle is found to be possible whenever the tension of the vesicle is not too large and the size of the particle neither too big *nor too small*. We then compare our simple variational calculations with solutions to the full Euler−Lagrange equations corresponding to the overall energy minimization and conclude that our results are qualitatively robust. For a physically reasonable set of membrane elasticity moduli and adhesion energies, we find an intermediate range of particle sizes for which the colloid is fully enveloped ("invaginated") by the vesicle—an obvious necessary prerequisite for endocytosis. For smaller sizes, there is no binding, and for larger ones, there is only partial wrapping. Full wrapping is assisted by a low membrane tension or large excess area, a condition that most likely holds for the plasma membrane of a cell but may not necessarily apply to intracellular membrane organelles, for example, endosomes. In the concluding discussion (section 5), we consider briefly several additional phenomena that are demonstrably important in the biological context. These involve the role of membrane proteins in controlling local spontaneous curvature and adhesion energies.

2. General Energy Considerations

The direct interaction of colloids with interfaces is due to several different factors, including, for instance, electrostatic, hydrophobic, or linker-molecule-mediated forces. We will not be specific about this point; instead, we assume that the direct interaction is well described by an adhesion energy, E_{ad}, that is proportional through an adhesion constant, k_{ad}, to the area of contact, A_{ad}, between the colloid and the interface:

$$E_{ad} = -k_{ad}A_{ad} \tag{1}$$

The assumption of a contact energy implies that the underlying microscopic force is rather short ranged. The hydrophobic attraction typically decays exponentially with a characteristic decay length of 1−2 nm.[9] In the case of linker molecules, the force range of course depends on the linker size. Electrostatic interactions, although in principle long-ranged, are comparatively local in biology because the omnipresent physiological salt concentration of about 100 mM monovalent salt leads to a Debye screening length of 1 nm, which is even smaller than the thickness of the lipid bilayer.

The reason that these attractive interactions usually do not lead to complete coverage of the colloid with the interface is that the formation of a contact area is counterbalanced by some sort of deformation of the interface. This will *increase* its energy because, if it were to lower it, the deformation would occur spontaneously (i.e., without the involvement of the colloid) and the original shape of the interface would be unstable.

For a stable interface, the surface energy must increase upon increasing its *area*, a fact related to the phenomenon of *surface tension*. When *surfactant* molecules are present, they reside preferentially at the interface and reduce its surface tension.[9,10] Furthermore, this surface energy is controlled by the concentration of surfactant in the bulk phase, which exerts its chemical potential, that is, acts as a reservoir. On the other hand, if the presence of surfactants in the bulk is essentially negligible, the number of them forming a particular interface may be regarded as constant on short enough time scales. Any change in the area of the interface will then lead to a change in the mean distance between surfactants and thus in their energy. Consequently, the surface tension will no longer be a material constant but will depend explicitly on the area itself.

Vesicles are closed interfaces formed by a self-assembled *bilayer* of surfactants, usually lipids. In this case, the two bulk phases separated by the membrane are often identical such that it is predominantly the interactions between these surfactants that are responsible for the surface energy. Assume that there is a particular area, A_l, at which these molecules are at an optimal separation and thus the surface at its lowest energy. Then, the surface tension depends not only on the actual area A, but also on the optimum lipid area A_l. In harmonic approximation, one may assume that the energy is proportional through k_{ten}—see eq 3—to the square of the difference between A and A_l.[11,12] For the wrapping problem, this has been discussed in ref 8, and we will summarize the main points in the next section.

Generally, a surface will also show resistance to *bending*, which means that its energy also depends on the local curvature. While it is clear that adhesion of a colloid onto a vesicle must lead to some sort of bending, and thus increase of energy, it is not obvious that this contribution will always oppose further wrapping. For instance, if one conceives of the strongly curved region at the colloid−vesicle contact as giving rise to a line tension, this contribution can support envelopment once the line has passed beyond the largest diameter of the colloid.

With two surface deformations that balance the adhesion, one must determine which of the two provides the dominant contribution. Below we will see that for large enough vesicles and colloids the surface tension will be the more important one. However, upon reducing the size of the colloids, vesicles, or both, curvature also becomes relevant. For typical curvature and adhesion constants, giant lipid vesicles and micron-sized colloids interact as if there is no curvature energy, but for smaller vesicles and in particular colloids of the size of viruses, the bending of the lipid bilayer strongly modifies the physics. It is the purpose of this article to discuss how in this case the joint interplay between adhesion, stretching, and bending energies determines the geometry of a colloid−vesicle complex.

Note that we refer to "energies" in the above discussion even though they invariably involve entropic contributions. Hydrophobic effects contribute to adhesion energies, for example, arising from water structure reorganization and attendant entropy decrease. Similarly, the stretching and bending energies of the vesicle are determined by changes in conformational disorder of the surfactant chains. In fact, integrating out microscopic degrees of freedom to arrive at a coarse-grained description always renders the remaining interactions "free energy" in nature. However, in our case, we prefer to use the term "energy" because there are entropic contributions on the *macroscopic* level that we will neglect. Most notable are the fluctuations of the lipid bilayer around its average shape, which give rise to an additional (but small) contribution to the surface tension (quite analogous to polymer elasticity, which is also of entropic origin). In this sense, we describe the problem on a macroscopic level as a balance between energy contributions, which derive from underlying microscopic degrees of freedom.

3. Balancing Adhesion and Stretching Energies

Recently, Dietrich, Angelova, and Pouligny performed the following conceptually simple experiment: they mixed latex spheres of a few micrometers in diameter with giant spherical unilamellar phospholipid vesicles of a few tens of micrometers in diameter.[8] Because of an effective attractive interaction between the two species, the latex spheres adhered to the vesicles and penetrated to some degree into their interior. One of the questions asked was what is the equilibrium geometry of the complex—see Figure 2.

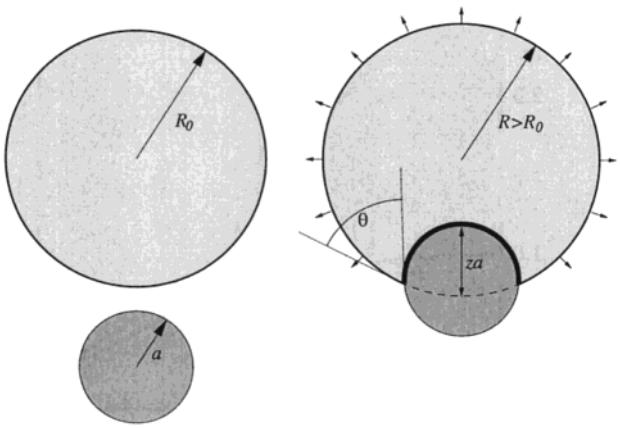

Figure 2. Schematic view of a colloid adhering to a spherical vesicle. In the complexed state, the contact area gives rise to a binding energy, while the resulting expansion of the vesicle requires work to be done against the membrane tension. The degree of penetration z and the contact angle θ are indicated as well.

Dietrich et. al[8] proposed a simple mathematical model for describing the equilibrium geometry of the complex. Because we extend their work here to include curvature effects, we need first to briefly discuss the original model.

The binding of the colloidal sphere to the large vesicle is described in terms of a balance between adhesion energy and tension within the vesicle membrane. The first is assumed to be proportional to the area of contact, $A_{ad} = 2\pi a^2 z$, and is given by eq 1. Here, z is the degree of penetration in units of the colloid radius a as illustrated in Figure 2. The tension opposing the wrapping ensues because pushing the colloid into the vesicle under the constraint of volume conservation[13] requires an expansion of the membrane area. At this point one has to pay attention to the actual state of the vesicle before adhesion. Generally, there is no equation relating surface and volume of a vesicle. If the volume is written as $V_0 = (4\pi/3)R_0^3$, then the surface area is at least $A_0 = 4\pi R_0^2$. Let A_l be the equilibrium area that the lipids forming the surface would occupy in a state of zero lateral tension, and define the *relative area excess*, ϵ, as

$$\epsilon = \frac{A_l - 4\pi R_0^{\,2}}{A_l} \tag{2}$$

A vesicle with a positive excess, $\epsilon > 0$, has more surface than necessary for closure, that is, the lipids need not be laterally pulled apart to accommodate the volume. For ϵ only slightly larger than zero, it is quasi-spherical. On the other hand, a vesicle with $\epsilon < 0$ can only enclose its volume if it expands its area beyond the value A_l by increasing the average separation between neighboring lipids beyond the optimal value. Such a vesicle exhibits a substantial membrane tension and is hence spherical.[14] In harmonic approximation, the tension energy is proportional to the square of the difference between the actual and the tensionless surface area, *if* the actual area is larger than the equilibrium area. Otherwise, the stretching energy may be regarded as zero, since − because of the relative smallness of the bilayer bending modulus − it is energetically more favorable to bend the membrane out of its original plane than to compress the lipids. This suggests

$$E_{ten} = \frac{1}{2}k_{ten}\frac{[\max\{A;A_l\} - A_l]^2}{A_l} \tag{3}$$

where k_{ten} is the surface expansion (lateral compressibility) modulus. The bilayer tension, σ, is then given by

$$\sigma = \frac{\partial E_{ten}}{\partial A} = k_{ten}\frac{\max\{A;A_l\} - A_l}{A_l} \tag{4}$$

After adhesion of a colloid, the shape of the vesicle is assumed to consist of two spherical caps with radius R ($\geq R_0$) and a—see Figure 2. The problem is now solved in three successive stages: First, find the geometry of the colloid−vesicle complex at a given penetration, z; in particular, find the new vesicle radius R (from the constraint of volume conservation). Second, compute the total energy $E_{ad} + E_{ten}$ using eqs 1 and 3. Third, minimize this with respect to z to obtain the equilibrium geometry.

Note that this curvature-energy-free model has only one characteristic length scale, for instance, all lengths can be scaled by the initial radius of the vesicle, R_0. This is a consequence of the fact that the two material constants, k_{ad} and k_{ten}, both have the same dimensions—energy per unit area. In addition to the area excess, ϵ, there are two more dimensionless variables that determine the physics of the problem: the ratio between the material constants and the ratio between the colloid and vesicle size. Let us define them to be

$$\zeta = k_{ad}/k_{ten} \quad \text{and} \quad \tilde{a} = a/R_0 \tag{5}$$

Figures 3 and 4 illustrate the prediction of the above model for the colloid penetration, z, and surface tension, σ, as a function of $\tilde{a}$, essentially reproducing the results from ref 8. The chosen material constants are $k_{ten} = 200$ dyn/cm [15]—typical for phospholipid bilayers, for instance, SOPC[11]—and $k_{ad} = 1$ erg/cm^2, which the authors of ref 8 obtain from their experiments. Note that in this case $\zeta = 5 \times 10^{-3}$ is a suitable smallness parameter.

Large colloids do not penetrate deeply because they give rise to a substantial tension. Upon reducing the colloid size, the penetration increases while the tension decreases. Finally, at $z = 2$, the colloid is fully wrapped—enveloped—and z remains at 2 for *all* smaller colloids. The tension shows a kink at this point and has the value $\sigma = k_{ad}/2$. Because the contact angle, θ, between the lipid bilayer and the colloid approaches zero there, this is seen as a consequence of the Young−Dupré equation, $\sigma(1 + \cos\theta) = k_{ad}$.[9,10] For even smaller values of a, penetration and contact angle remain at 2 and 0, respectively, but because the final state is no longer a balance between adhesion and tension (adhesion is always stronger, but there is no surface left to be wrapped), the Young−Dupré equation no longer applies.

If the initial vesicle has excess area, it can wrap the sphere more easily. Hence, the penetration, z, is larger compared to the case with zero excess area ($\epsilon = 0$), and the membrane tension is lower (see dashed curves in Figures 3 and 4). Conversely, if the vesicle is already under pretension due to lack of area, the penetration is lower and the tension is larger (dotted curves); in the case shown, full wrapping ($z = 2$) is impossible even in the limit $\tilde{a} \to 0$. Generally, the point of wrapping is given by[8,16]

$$\tilde{a} = x^{1/2} - \frac{1}{3}x + \frac{5}{18}x^{3/2} \mp \cdots \quad \text{with} \quad x = \frac{\zeta/2 + \epsilon}{1 - \epsilon} \tag{6}$$

Among other things, this shows that full wrapping is impossible if the lack in vesicle area is such that $\epsilon < -\zeta/2$ ($= -0.25\%$ in the present example), explaining why the dotted curve in Figure 3 never reaches $z = 2$.

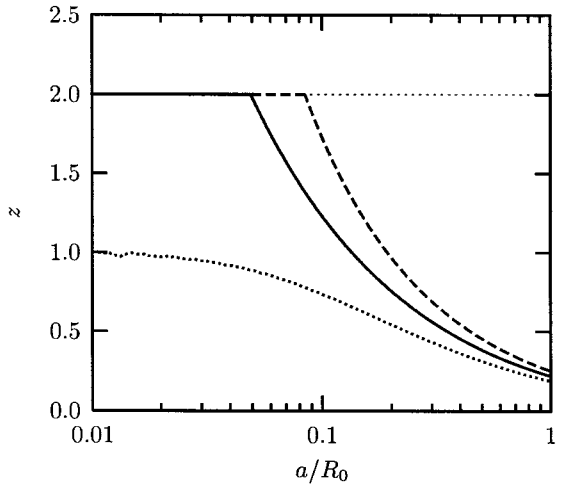

Figure 3. Penetration, z, as a function of the ratio $\tilde{a} = a/R_0$ of colloid size and initial vesicle size. The lines correspond to $\epsilon = 0$ (solid), $\epsilon = +0.5\%$ (dashed), and $\epsilon = -0.5\%$ (dotted). The material constants were chosen as $k_{ad} = 1$ erg/cm^2 and $k_{ten} = 200$ dyn/cm.[15]

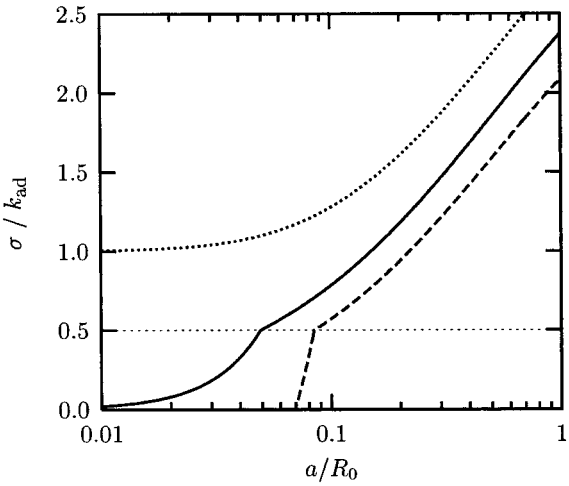

Figure 4. Vesicle tension σ from eq 4 in units of k_{ad} calculated as a function of $\tilde{a}$. The material constants and the line styles correspond to the three cases shown in Figure 3.

The authors of ref 8 present a comparison of the experimentally determined penetration with the results of the simple theoretical model, from which they also determine the value of the adhesion constant, k_{ad}. They conclude that their model gives a good explanation of the observable geometry of the adhesion complex; in particular, the dependence of the contact angle θ on the size ratio a/R_0 (which is a consequence of the tension increasing with penetration and which would not apply to a simple wetting scenario) is well reproduced.

In the following, we show that the incorporation of curvature effects results in the appearance of a new length scale. Only if this is small compared to all other lengths in the problem can the curvature contribution be neglected.

4. Including Curvature Energy

4.1. Restricted Variational Formulation. Membranes show a resistance to bending. A widely used expression for this curvature energy per unit area in harmonic approximation has been given by Helfrich[12]

$$e_c = \frac{1}{2}k_c(\kappa_1 + \kappa_2 - 2c_0)^2 + \bar{k}_c\kappa_1\kappa_2 \qquad (7)$$

where κ_1 and κ_2 are the principal curvatures (i.e., inverse principal radii), c_0 is the spontaneous curvature, and k_c and $\bar{k}_c$ are two curvature moduli (called the bending and the saddle-splay modulus[17]). The first term measures the quadratic deviation of the mean curvature, $(\kappa_1 + \kappa_2)/2$, from the spontaneous curvature, c_0, while the second term is the contribution of the Gaussian curvature, $\kappa_1\kappa_2$. The total curvature energy, E_c, of the vesicle is the surface integral over eq 7:

$$E_c = \oint \mathrm{d}A\, e_c \qquad (8)$$

As a consequence of the Gauss−Bonnet theorem from differential geometry, integrating the Gaussian curvature over a closed surface yields a topological invariant.[18] Because we will not consider topological changes of the vesicle, the second term in eq 7 will thus only contribute a constant to the energy, which we can ignore. Furthermore, because we study symmetric lipid bilayers, the spontaneous curvature, c_0, is equal to zero. Hence, there is only one new physical quantity in our problem—the bending modulus, k_c.

The new elastic constant has the dimensions of an energy and permits the definition of a new length scale, λ, according to

$$\lambda = \sqrt{k_c/k_{ad}} \qquad (9)$$

For a typical value of $k_c = 20k_BT$[19] and the same adhesion constant, $k_{ad} = 1$ erg/cm^2, as applied above, this length is about 10 nm. This is much smaller than the sizes of the colloids and vesicles considered in ref 8, and consequently, these authors argue that curvature effects are negligible in their situation. However, there exist important situations in which the wrapping of colloids by membranes occurs on length scales that are much smaller. One example, already featured in the Introduction, is the phenomenon of *endocytosis*,[1,4] the mechanism by which an object gets from one side of a fluid lipid membrane to the other via a wrapping and subsequent fission process, see Figure 1. In particular, it is believed that the final stage in the maturation of type-D retroviruses consists of the wrapping of the viral core particle (which is preassembled in the cytoplasm) by the plasma membrane of the host cell.[6,7] These viruses have a diameter of about 80−100 nm, so the radius of curvature of their enveloping membrane is comparable to the length scale λ.

For the reasons outlined above, we would like to incorporate curvature effects into the description of the vesicle. The complete way of finding the minimum-energy solutions of this problem is to consider the energy as a functional of the shape of the vesicle and to minimize with respect to the shape. One would then, for instance, have to solve the corresponding Euler−Lagrange equations under constraints such as volume and area conservation. For the case of axisymmetric vesicles with fixed volume and area, one obtains a fourth-order nonlinear ordinary differential equation, volume and area being fixed by Lagrange multipliers. The rich phase diagram of vesicle conformations that arise has been studied thoroughly in the past—see, for instance, the review by Seifert.[20]

In our work, we also restrict ourselves to axisymmetric colloid−vesicle complexes, but we will not, in general, solve the full shape equations. For initially spherical vesicles, we present a simple extension of the model from section 3 by introducing one more variational parameter, which describes an averaged radius of curvature near the contact line. For this model, we present a phase diagram (see section 4.2) that distinguishes the three different stages of adhesion: free, partially wrapped, and enveloped.

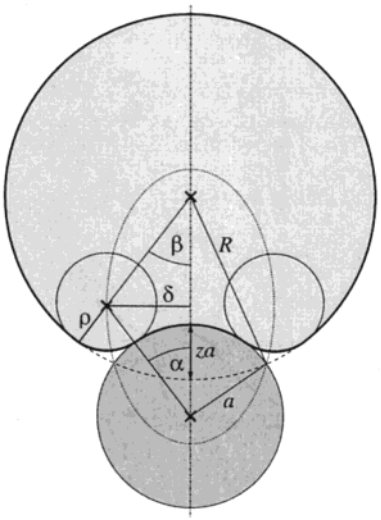

Figure 5. Two-parameter ansatz for the shape of the colloid−vesicle complex. In addition to the penetration z, we introduce the radius ρ of the rounded contact line, which is modeled as part of a toroid. Equivalently, we can use the two radii δ and ρ of the toroid for parametrizing the shape. The dotted ellipse is the location of the midpoints of all possible circles that touch the two circles with radii a and R.

We will also study briefly (section 4.3) the *full* variational problem by solving the shape equations for vesicles adhering on spheres for a few typical situations. In this case, however, we will not consider laterally extensible membranes but rather assume the area to be fixed. It will nevertheless give us a way of testing the assumptions about vesicle geometry made in our restricted variational approach.

Let us consider then a simple extension of the adhesion model proposed in ref 8. If we assume that the most significant difference in the vesicle shape occurs at the contact line, which has to be rounded rather than kinked, we are led to an "ansatz" for the vesicle shape as pictured in Figure 5. We will assume that the vesicle surface consists of an upper spherical cap with radius R, a lower spherical cap of radius a, equal to the radius of the adhering colloid, and a rounded region between, which we model as part of a torus with radii δ and ρ. The interpenetration between the a- and the R-circle is za, that is, the distance between their midpoints is $R + a - za$.

In Appendix A, we establish geometrical relations between these quantities and show how all geometric properties of interest, for example, total area A and volume V of the vesicle or the adhesion area A_{ad}, can be written as explicit functions of R, a, δ, and ρ. The excess curvature energy is proportional through k_c to the difference between the integrated squared mean curvatures of the final and the initial vesicle

$$\Delta E_c = 2k_c \Delta C_m^{\ 2} \tag{10}$$

This difference ΔC_m^2 is evaluated in Appendix B—see eq 32. In this way, one can calculate the excess curvature energy as an explicit function of α, β, δ, and ρ (where the former two are themselves functions of the latter two). Finally, the geometry is optimized by finding those values of δ and ρ that at given vesicle volume lead to the lowest total energy.

4.2. Structural Phase Diagrams. Let us discuss first the results that we obtain from solving the two-parameter model of the vesicle. We study adhesion of a colloidal sphere onto an initially spherical but tensionless vesicle, that is, the area excess, ϵ, defined in eq 2 is zero. For the purpose of illustration, we will use the same adhesion and membrane stretching constants as ref 8. For the membrane bending modulus, we choose the value $k_c = 20k_BT$, which is typical for phospholipid bilayers; as remarked earlier, these choices imply $\zeta = 5 \times 10^{-3}$ and $\lambda \approx 9$ nm.

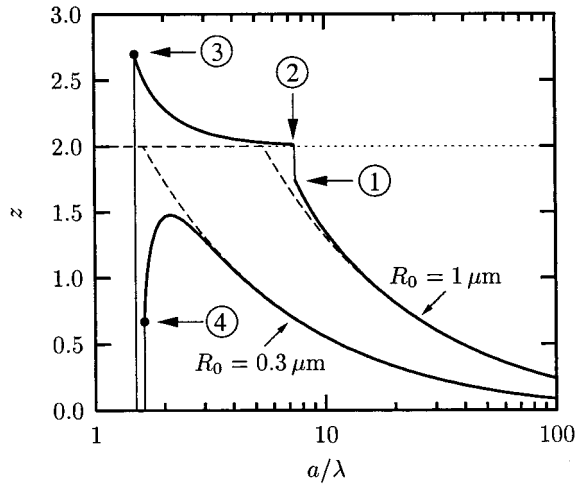

Figure 6. Equilibrium penetration z as a function of colloid size a for two different initial vesicle radii R_0. The solid and dashed lines correspond to the cases with and without curvature contribution, respectively. The material constants have been chosen as $k_{ad} = 1$ erg/cm^2, $k_{ten} = 200$ dyn/cm, and $k_c = 20k_BT$, which implies that the characteristic length from eq 9 has the value $\lambda \approx 9.07$ nm. Four particular configurations, indicated by arrows, are visualized in Figure 8.

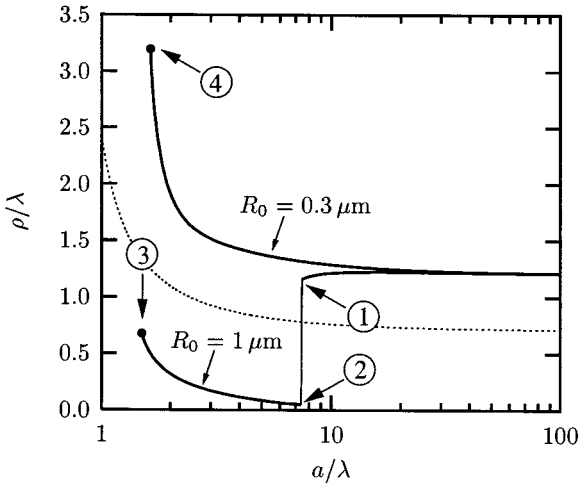

Figure 7. Equilibrium radius ρ of the toroidally rounded contact line as a function of colloid size a for the same two different initial vesicle radii R_0 and the same material constants as in Figure 6. The dotted line indicates the radius of curvature at contact as it applies to the full variational problem, eq 11 (see also Appendix C). The numbered arrows match the ones from Figure 6.

Figure 6 shows the penetration z as a function of colloid size a for two different initial vesicle radii R_0. For comparison, the results from the case neglecting curvature energy are included as dashed lines. The corresponding toroidal radii ρ are shown in Figure 7. As expected, for sufficiently large colloid radii a, the model without curvature energy gives a very good description of the penetration; but if a is no longer large compared to λ, deviations occur that can lead to two qualitatively different scenarios. If the initial vesicle radius R_0 is large enough, the penetration z jumps discontinuously to the value 2 at some critical colloid size $a > (R_0)$—the vesicle envelops the colloid completely (transition 1 → 2). Actually, the penetration is found to be slightly larger than 2 because the toroid radius ρ, although

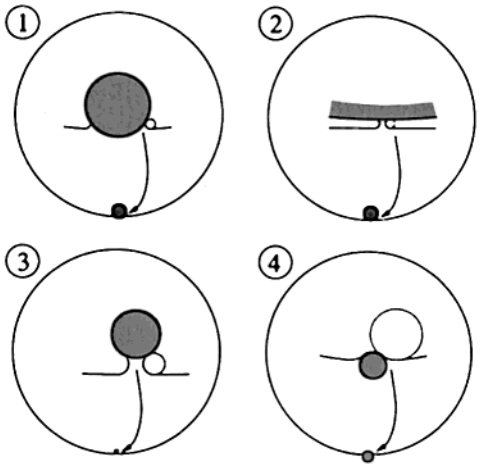

Figure 8. Shape of the four colloid−vesicle complexes pointed out by the numbered arrows in Figures 6 and 7. The insets enlarge the region around the colloid, and the dotted circles indicate the crossection of the contact toroid with radius ρ. Note that the four pictures are not drawn to the same scale.

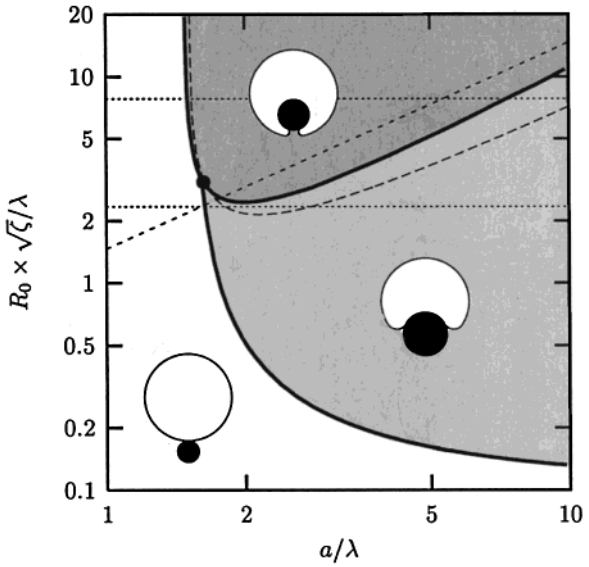

Figure 9. Phase diagram of colloid−vesicle complexes in the $(a;R_0)$ plane. The white, light gray, and dark gray regions correspond to unbound, partially wrapped, and enveloped states, respectively, as also indicated qualitatively by the little pictures. The short-dashed line is the phase boundary from the case in which curvature energy is neglected—eq 6—dividing the partially wrapped state (below) from the enveloped one (above). The long-dashed curve is the result of the navel solution eq 14, which also suggests the scaling of the two axes. The two horizontal dotted lines indicate the a-scans that have been shown in Figures 6 and 7.

dropping significantly at the transition (see Figure 7), is still nonzero at the neck, as can be seen in picture 2 of Figure 8. We note that (1) the inclusion of the bending energy can lead to an *increased* penetration and (2) that $z > 2$ is impossible in the description that neglects a rounding of the contact region. If we reduce further the size of the colloid, the penetration increases even more. This is a direct result of an increasing toroid radius ρ, which itself is related to the fact that within the full variational problem the contact curvature can be shown to decrease with increasing substrate curvature according to[21,22]

$$c^* = \sqrt{\frac{2k_{ad}}{k_c}} + c_s = \frac{\sqrt{2}}{\lambda} + c_s \qquad (11)$$

where c_s is the meridianal substrate curvature, which in our case is simply $-1/a$. Some brief remarks on the relation between the theoretical contact curvature and the torus radius ρ can be found in Appendix C. Going to even smaller values of a, we finally reach a lower critical value $a_<(R_0)$, at which the penetration discontinuously drops back to values smaller than 2. For most values of R_0, this transition results in complete unbinding of the colloid (i.e., $z = 0$), as is also the case for the example in Figure 6 (arrow 3). However, for a small range of vesicle radii the colloid ceases to be enveloped slightly below $a_<(R_0)$ remaining partially wrapped until unbinding occurs at an even smaller radius $a_u(R_0)$. Both transitions arise because the energy gain due to adhesion can no longer compensate for the cost of bending and stretching the membrane. Thus, colloids smaller than a_u do not bind to the vesicle, while colloids in the range $[a_<; a_>]$ are fully enveloped.

If the vesicle radius R_0 is too small, the penetration will not reach a value $z > 2$ for any colloid radius. This is the case for the second curve in Figure 6 with $R_0 = 0.3\ \mu$m. But again, colloids that are too small will not bind to the vesicle at all (see arrow 4 in Figure 6). Because the tension contribution becomes more important for decreasing vesicle radii, $a_u(R_0)$ monotonically increases with decreasing R_0.

The above findings may be summarized in a structural phase diagram, which marks the three states of a colloid−vesicle complex (free, partially wrapped, and enveloped) for different values of colloid and vesicle radius; this is shown in Figure 9 for the material constants used above. Within our model, the three phase boundaries correspond to discontinuous changes in shape properties, such as the penetration. There also exists a triple point at which all three states have the same energy. Its coordinates for the given material constants are $(a_t/\lambda; R_{0,t}\sqrt{\zeta}/\lambda) \approx (1.61; 3.13)$. The phase boundary $a_u(R_0)$ has a kink at the triple point, while $a_<(R_0)$ is smooth. Both lines coincide for $R_0 > R_{0,t}$. The two a-scans from Figures 6 and 7 correspond to horizontal lines in Figure 9, which either pass through the dark-gray shaded enveloped region (for $R_0 = 1\ \mu$m) or miss it below (for $R_0 = 0.3\ \mu$m). The phase boundary in the original model neglecting curvature energy is given by eq 6, which separates the partially wrapped (below) from the enveloped (above) state and is a straight line in the (a, R_0) plane—see short-dashed line. It merges asymptotically but slowly with the phase boundary of the curvature case for $a \to \infty$ because in this limit the vesicle geometry is determined by the balance between tension and adhesion and curvature is only a small perturbation.

In the enveloped case $z > 2$, the toroid radius is found to be very small. Picture 2 in Figure 8 shows that the contact region essentially consists of the inner half of a toroid. The excess integrated squared mean curvature should therefore be well approximated by eq 33, which only depends on the ratio δ/ρ of the two toroid radii. Because the toroid is small again, it is reasonable to look at the limit $\delta \to 0$ and $\rho \to 0$ such that the ratio stays at its optimal value $\delta/\rho = 1.59845$ (see Appendix B); the contact line then shrinks to a navel point with an energy of about $3.79k_c$. The constraint of volume conservation is given in this same limit by $R_0^3 = R^3 - a^3$, and the vesicle area is $A = 4\pi R_0^2[(1 + \tilde{a}^3)^{2/3} + \tilde{a}^2]$ with $\tilde{a} = a/R_0$. For $\epsilon = 0$, the total energy is found to be

$$E = 2\pi R_0^2 k_{ten}\left\{[(1+\tilde{a}^3)^{2/3} + \tilde{a}^2 - 1]^2 - 2\zeta\tilde{a}^2 + 4.603\frac{\zeta\lambda^2}{R_0^2}\right\} \qquad (12)$$

The last term is the contribution from the navel. Up to quartic order in $\tilde{a}$, the total energy above can be written as

$$\frac{E}{2\pi {R_0}^2 k_{\text{ten}}} = \tilde{a}^4 - 2\xi\tilde{a}^2 + 4.603\frac{\xi\lambda^2}{R_0^2} \qquad (13)$$

A comparison with results from the variational ansatz shows that eq 12 gives an excellent description of the complex energy within the range of envelopment, $[a_<; a_>]$. For instance, for $R_0 = 1\ \mu$m, the navel approximation predicts an energy at the point $a_>$, which is only about half of a k_BT larger than the true solution, involving a relative deviation of 7×10^{-5}. Because enveloped colloids are well described by this ansatz, it yields a simple way of determining the point of unbinding, namely, by setting the navel energy to zero. Using the quartic approximation, we thus obtain

$$R_0\sqrt{\xi}/\lambda = \frac{(a/\lambda)}{\sqrt{2 - 4.603(\lambda/a)^2}} \qquad (14)$$

This function is plotted as a long-dashed curve in the phase diagram of Figure 9. As expected, it gives a very good description of the unbinding phase boundary above the triple point. Surprisingly though, it also reproduces the qualitative shape of the wrapping boundary, although this line is given by the energy balance between an enveloped and a partially wrapped state rather than a free state. However, the large-a behavior $a/R_0 \sim \sqrt{2\xi}$ is only a factor 2 off from the correct asymptotic behavior of the model neglecting curvature energy, eq 6. Localizing the position of the minimum, one finds $a/\lambda = R_0\sqrt{\xi}/\lambda = \sqrt{4.603} \approx 2.15$, suggesting that vesicles with radii smaller than $2.15\lambda/\sqrt{\xi}$ will not envelop any colloid. Although our simplified ansatz will not give reliable prefactors, the scaling of the minimal vesicle radius with $\lambda/\sqrt{\xi} = \sqrt{k_c k_{\text{ten}}}/k_{\text{ad}}$ is probably correct.

Equation 14 diverges for $a \simeq 1.52\ \lambda$, showing (1) that no smaller colloid can bind to the vesicle and (2) that this is exclusively due to curvature effects because λ does not depend on the surface expansion modulus, k_{ten}.

4.3. Full Solution of the Variational Problem. In this final part, we would like to briefly discuss a few aspects of the full variational problem, in which the energy is considered as a functional of the vesicle shape. The latter is then determined by solving the corresponding Euler−Lagrange equations, as outlined in detail, for instance, in ref 23. At the membrane−colloid contact boundary, conditions have to be satisfied guaranteeing that the membrane approaches the colloid with zero contact angle and that at contact the principal curvature c^* along the meridian is given by eq 11. For simplicity, we solve the shape equations for inextensible membranes under the constraint of fixed surface area and volume by adding the terms $\sigma(A - A_0)$ and $P(V - V_0)$ to the energy functional, where σ and P correspond to surface tension and pressure, respectively. One may then compare a given solution of the full variational problem with a solution of the simpler model, in which the membrane expansion modulus, k_{ten}, has been adjusted to yield the same surface tension.

Figure 10 shows the result of such a comparison. The left picture is the full solution of the shape equations for constants $a = 45$ nm, $R_0 \approx 84.2$ nm, $k_{\text{ad}} = 1$ erg/cm^2, and $k_c = 20k_BT$. The surface tension is found to be $\sigma \approx 0.8829$ dyn/cm. By choosing the membrane expansion modulus as $k_{\text{ten}} \approx 70.44$ dyn/cm, the simple two-parameter variational calculation gives an equilibrium colloid−vesicle complex with the same surface tension. Its form is shown in the right picture of Figure 10. While both shapes agree very well qualitatively, the full variational problem gives a somewhat smoother appearance because the relatively large curvature of the rounded contact region changes continuously to the smaller curvature of the spherical vesicle cap. Performing an extrapolation of this cap permits the definition of the penetration z in the full case just as before, giving $z \approx 0.582$, while the two-parameter variation gives the slightly smaller $z \approx 0.484$. The similarity between the two shapes indicates that our variational ansatz captures the essential features of the case including curvature energy. We therefore consider our results as qualitatively robust while, of course, not quantitatively precise.

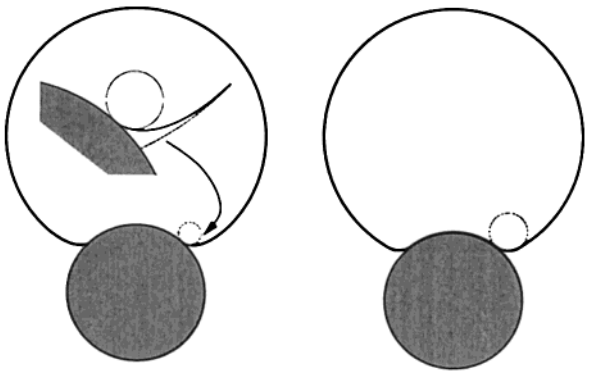

Figure 10. Comparison of colloid−vesicle complexes determined from the full variational problem (left) and from the simpler two-parameter ansatz (right), which coincide in their values of a, R_0, k_{ad}, and σ (see text). In each case, the dotted circle shows the radius of curvature at contact, $1/c^*$; in the right figure, the curvature radius is constrained to remain at this value all the way up to the point where it (discontinuously) switches to R. The inset in the left figure magnifies the region around the contact; the dashed line there is an extrapolation of the spherical vesicle cap.

Finally, we note that the full variational approach enables the study of *flaccid* vesicles. Because their overall shape is not spherical, they are not well described by our simplified ansatz. As an example, Figure 11 compares the picture of an experimentally observed colloid−vesicle complex[24] with a stationary shape obtained from the full variational problem. In the experiment, giant unilamellar phospholipid vesicles (made of POPC or DMPC) were mixed with latex beads that were chemically grafted with streptavidin—a water soluble protein that specifically binds to biotin. Adhesion of the bead was induced by including biotinilated lipids into the vesicle, and the complex was observed in differential interference contrast microscopy. The striking similarity between the observed and the calculated conformations suggests that a theoretical description of these shapes using the full shape equations is appropriate. It may, for instance, be used to infer structural information about the region close to the colloid−membrane contact, which is difficult to get from the image. However, a full study of the structural phase diagram describing colloid−vesicle complexes using the shape equations is numerically involved and beyond the aim of this paper.

5. Discussion

We have presented above a simple theory that treats systematically the competing effects of adhesion energy and bilayer elastic moduli—both stretching and bending—in determining the extent of wrapping of a colloidal particle by a model membrane. We distinguish between three states of the particle/membrane complex: (1) partially wrapped, (2) fully enveloped,

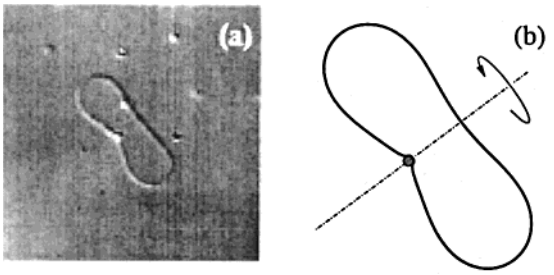

Figure 11. The left picture shows an experimentally observed colloid−vesicle complex (reproduced with permission from ref 24. Koltover, I.; Rädler, J. O.; Safinya, C. R. *Phys. Rev. Lett.* **1999**, *82*, 1991. Copyright 1999 by the American Physical Society.); the right picture shows the shape of a stationary solution of the full variational problem for a flaccid vesicle with a large excess area (about 22%). The colloid radius in both pictures is 0.45 μm. For the theoretical calculation, the values $k_c = 20k_BT$ and $k_{ad} = 7.8 \times 10^{-4}$ erg/cm^2 have been used. Furthermore, $V_0 \approx 3.45 \times 10^3$ μm^3, $A_0 \approx 1.35 \times 10^3$ μm^2 and $\alpha \approx 0.354\pi$.

and (3) unbound. A structural phase diagram is derived as a function of particle (a) and vesicle size (R_0). For physically reasonable values of adhesion energy and bilayer moduli, two basic scenarios are found upon, say, decreasing the size of the colloidal particle. For large enough vesicles, decreasing a leads first to progressively more wrapping, then to a discontinuous jump to fully enveloped particles, and finally to an unbinding (again discontinuous) of the complex. For smaller vesicles, full envelopment is never achieved, but rather the trend of increasing wrapping upon size reduction of the particle reverses at some point until the particle finally unbinds. Predictions of the crossover between the various regimes are obtained in terms of the basic adhesion and elasticity energies, suggesting several possible experiments for testing these ideas with well-characterized colloidal particles and unilamellar vesicles.

What about the connection of these results to the biological context? Invariably, both endo- and exocytosis processes involve the "recruitment" of membrane proteins in facilitating the adhesion between particle and membrane. In the case of viruses, for example, the particle enters only because its ligands bind specifically to receptors in the outer-membrane leaflet, thereby initiating the signaling cascade necessary for endocytosis.[1] In particular, the ligand−receptor interaction induces an active process in which a network of clathrin molecules is formed on the *inner* leaflet of the cell membrane. This network has a spontaneous curvature associated with it that facilitates the wrapping of the membrane around the viral particle. At the end of the infection cycle, when a large number of viral particles have been replicated, each one must leave the cell by an exocytosis event. This exit process appears to be simpler, in general, than that of initial entry, because no specific recognition step need be involved. Nevertheless, membrane proteins still play a key role in driving the wrapping and envelopment of the viral core particle.[7] But in this instance, they are membrane proteins encoded by the *viral* genome, and they bind directly to the viral capsid. Their local accumulation in the membrane is driven by their binding to the capsid, but it is not clear whether their role is to enhance the adhesion or to lower the effective bending energy by inducing the appropriate spontaneous curvature. It is even conceivable that the mere presence of a line tension between the coated and uncoated regions of the membrane efficiently promotes the budding process.[25] Accordingly, theory along the lines that we have formulated above needs to be extended to include the important "extra" degree of freedom provided by the membrane proteins, that is, an adhesion and spontaneous curvature that depend on the local concentration of proteins in the membrane.

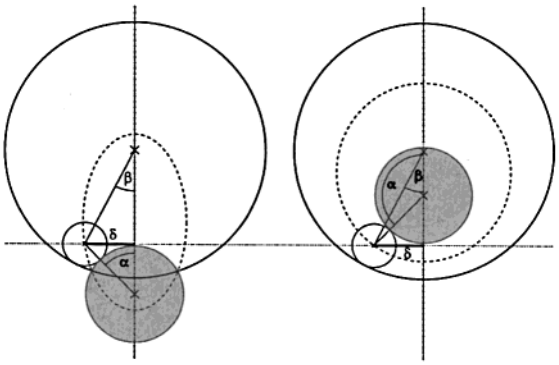

Figure 12. Lower solution ($\alpha \le \pi/2$; left) and upper solution ($\alpha \ge \pi/2$; right) for the system of equations (15−17) at given values of δ and ρ.

Acknowledgment. We have benefitted from many stimulating discussions with Pierre Sens and with Avinoam Ben-Shaul in the early stages of this work. M.D. also gratefully acknowledges financial support by the Deutsche Forschungsgemeinschaft (DFG) under Grant De775/1-1. This work is partially supported by National Science Foundation Grant No. CHE9988651 to W.M.G.

Appendix A. Geometrical Relations in the Restricted Variational Problem

As can be seen in Figure 5, the toroid circle with radius ρ has to touch both of the other two intersecting circles with radii R and a. Its midpoint therefore has to lie on the ellipse that has the two midpoints of the other circles as foci and that has a major axis of length $R + a$. This is easily seen by recalling that the distance d from one focus to the other focus via any point P on the ellipse is independent of P and equal to the length of the major axis. If one chooses P to be the midpoint of the torus circle with radius ρ, the double-touching condition implies $d = (R - \rho) + (a + \rho) = R + a$, which is independent of ρ and fixes the major axis.

Let us introduce the two angles α and β according to Figure 5. Using them, we can immediately write down the following three equations:

$$\delta = (a + \rho) \sin \alpha \tag{15}$$

$$\delta = (R - \rho) \sin \beta \tag{16}$$

$$R + a - za = (a + \rho) \cos \alpha + (R - \rho) \cos \beta \tag{17}$$

The first two equations specify α and β but for the ambiguity of whether they are in the range $[0;\pi/2]$ or $[\pi/2;\pi]$. In principle, this results in four cases, but the only physically significant solutions are those for which $\beta < \pi/2$ and either $\alpha \le \pi/2$ ("lower solution") or $\alpha \ge \pi/2$ ("upper solution"), see Figure 12. Insertion into eq 17 gives z as a function of δ, ρ, and the two radii R and a:

$$R + a - za = \pm\sqrt{(a + \rho)^2 - \delta^2} + \sqrt{(R - \rho)^2 - \delta^2} \tag{18}$$

where the $\pm$ sign corresponds to the lower (+) or the upper (−) solution.

We also need to know the total area and volume of the vesicle. Using eq 25, we find the area

$$A = 2\pi\Big\{R^2(1+\cos\beta) + a^2(1-\cos\alpha) + \delta\rho\Big[\alpha+\beta+\frac{\rho}{\delta}(\cos\alpha-\cos\beta)\Big]\Big\} \quad (19)$$

From this follows the surface tension energy via eq 3. The area of adhesion between the vesicle and the colloid is given by

$$A_{ad} = 2\pi a^2(1-\cos\alpha) \quad (20)$$

and the adhesion energy is again calculated by eq 1.

To satisfy the constraint of fixed vesicle volume, we need to use (see eq 26 in Appendix B)

$$V = \frac{2\pi}{3}\Big\{R^3(1+\cos\beta) - a^3(1-\cos\alpha) + \frac{\delta^2}{2}(R+a-za) + \delta\rho^2\Big[\frac{3}{2}(\alpha+\beta)+\cos\alpha-\cos\beta\Big]\Big\} \quad (21)$$

Appendix B. Some Differential Geometry of the Toroid

In this appendix, we include some basics relevant to describing the curvature of the toroidal part of the vesicle. For more details of the underlying differential geometry, we refer the reader to DoCarmo.[18]

Our choice of coordinates for a toroid is illustrated in Figure 13. For any given toroid radii δ and ρ, the surface is mapped by the two angles φ_1 and φ_2. The position vector in toroidal coordinates is thus

$$\mathbf{r} = \begin{pmatrix}(\delta-\rho\sin\varphi_1)\cos\varphi_2\\(\delta-\rho\sin\varphi_1)\sin\varphi_2\\\rho\cos\varphi_1\end{pmatrix} \quad (22)$$

The first fundamental form g of the surface (i.e., the surface metric) is given by

$$\mathbf{g} = \frac{\partial\mathbf{r}}{\partial\varphi_i}\cdot\frac{\partial\mathbf{r}}{\partial\varphi_j} \equiv \begin{pmatrix}\rho^2 & 0\\0 & (\delta-\rho\sin\varphi_1)^2\end{pmatrix} \quad (23)$$

The area element, dA, is thus given by

$$\mathrm{d}A = \sqrt{\det\mathbf{g}}\,\mathrm{d}\varphi_1\,\mathrm{d}\varphi_2 = \rho(\delta-\rho\sin\varphi_1)\,\mathrm{d}\varphi_1\,\mathrm{d}\varphi_2 \quad (24)$$

and the volume element is simply $\mathrm{d}V = \mathrm{d}A\,\mathrm{d}\rho$. From this, we find the area, $A(\bar\varphi_1)$ of the rotationally symmetric patch $[0;\bar\varphi_1] \times [0;2\pi]$,

$$A(\bar\varphi_1) = \int_0^{\bar\varphi_1}\mathrm{d}\varphi_1\int_0^{2\pi}\mathrm{d}\varphi_2\,\rho(\delta-\rho\sin\varphi_1) = 2\pi\rho[\delta\bar\varphi_1 - \rho(1-\cos\bar\varphi_1)] \quad (25)$$

and the corresponding volume, $V(\bar\varphi_1)$, of the underlying part of the torus within the same range of angles,

$$V(\bar\varphi_1) = \pi\rho^2\Big[\delta\bar\varphi_1 - \frac{2}{3}\rho(1-\cos\bar\varphi_1)\Big] \quad (26)$$

The normal vector to the surface is given by

$$\hat{\mathbf{n}} = \frac{\partial_{\varphi_1}\mathbf{r}\times\partial_{\varphi_2}\mathbf{r}}{|\partial_{\varphi_1}\mathbf{r}\times\partial_{\varphi_2}\mathbf{r}|} = \begin{pmatrix}\sin\varphi_1\cos\varphi_2\\\sin\varphi_1\sin\varphi_2\\-\cos\varphi_1\end{pmatrix} \quad (27)$$

from which we find the second fundamental form

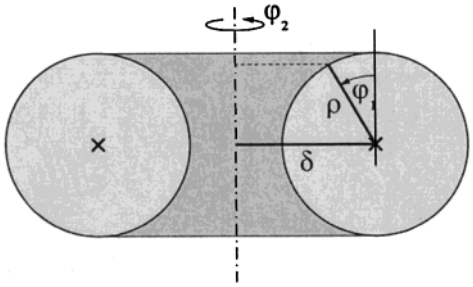

Figure 13. Choice of coordinates for the toroid.

$$\mathbf{N} = \frac{\partial\hat{\mathbf{n}}}{\partial_{\varphi_i}}\cdot\frac{\partial\mathbf{r}}{\partial_{\varphi_j}} \equiv \begin{pmatrix}-\rho & 0\\0 & (\delta-\rho\sin\varphi_1)\sin\varphi_1\end{pmatrix} \quad (28)$$

The local Gaussian curvature, c_G, is then given by

$$c_G \equiv \kappa_1\kappa_2 = \frac{\det\mathbf{N}}{\det\mathbf{g}} = \frac{-\sin\varphi_1}{\rho(\delta-\rho\sin\varphi_1)} \quad (29)$$

The two principal curvatures, κ_1 and κ_2, are now easily determined because evidently one of the principal radii of curvature is given by ρ. Hence, we obtain

$$\kappa_1 = \frac{1}{\rho} \quad \text{and} \quad \kappa_2 = \frac{-\sin\varphi_1}{\delta-\rho\sin\varphi_1} \quad (30)$$

For the curvature energy, we need the integral over the square of the local mean curvature, $c_m(\varphi_1) = {}^1/_2(\kappa_1+\kappa_2)$ for the patch $[0;\bar\varphi_1] \times [0;2\pi]$:

$$C_m{}^2(\bar\varphi_1) = \int_0^{\bar\varphi_1}\int_0^{2\pi}\mathrm{d}A\,c_m{}^2 \quad (31)$$

In addition to the toroidal "rim", the integrated squared mean curvature of the *full* vesicle also contains the contributions from the two spherical caps with radii a and R and opening angles α and $\pi-\beta$ (cf. Figure 5). For the initial vesicle, we restrict ourselves to the case of zero area excess ($\epsilon = 0$), which implies a spherical geometry. Combining all of these terms and evaluating the integral from eq 31, we obtain the *excess* curvature energy from eq 10 as an explicit function of the vesicle geometry, with the form of $\Delta C_m{}^2$ depending on which of the two toroid radii is larger:

$$\begin{aligned}\Delta C_m{}^2 &= \oint_{\text{new vesicle}}\mathrm{d}A\,c_M{}^2 - 4\pi\\ &= 2\pi(1+\cos\beta) + 2\pi(1-\cos\alpha) + C_m{}^2(\alpha) - C_m{}^2(-\beta) - 4\pi\\ &= \frac{\pi(\delta/\rho)^2}{\sqrt{|(\delta/\rho)^2-1|}}\times\\ &\begin{cases}\arctan\dfrac{1+(\delta/\rho)t_\beta}{\sqrt{(\delta/\rho)^2-1}} - \arctan\dfrac{1-(\delta/\rho)t_\alpha}{\sqrt{(\delta/\rho)^2-1}} & \text{for } \delta > \rho\\ \dfrac{1}{2}\ln\left(\dfrac{t_\alpha - t_\beta - \sqrt{1-(\delta/\rho)^2}(t_\alpha+t_\beta) + (\delta/\rho)(t_\alpha t_\beta - 1)}{t_\alpha - t_\beta + \sqrt{1-(\delta/\rho)^2}(t_\alpha+t_\beta) + (\delta/\rho)(t_\alpha t_\beta - 1)}\right) & \text{for } \delta < \rho\end{cases}\end{aligned} \quad (32)$$

where $t_\alpha = \tan(\alpha/2)$, $t_\beta = \tan(\beta/2)$. The second expression follows from the first by using the identity $-i\arctan(ix) = a\tanh x = {}^1/_2\ln[(1+x)/(1-x)]$. We will also need the case in which $\alpha \to \pi^-$ and $\beta \to 0^+$:

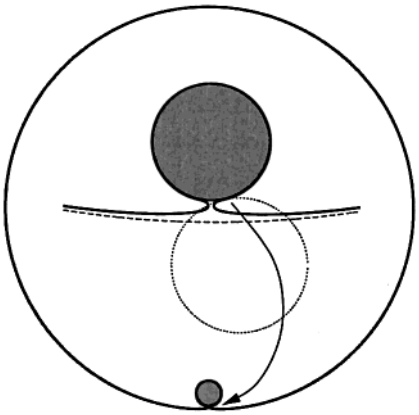

Figure 14. Shape of a stationary colloid−vesicle complex determined from the full variational problem under the constraint of fixed volume and area. The physical constants are $k_{ad} = 1$ erg/cm^2, $k_c = 20k_BT$, $a =$ 12 nm, $R_0 \approx 192$ nm, and $A_0 \approx 4.65 \times 10^5$ nm^2. In this case, $A_0 = A_l$, which gives a relative area excess $\epsilon \approx 0.4\%$. The inset shows a magnification of the region around the neck. Observe that the radius of curvature at *contact* (as indicated by the dotted circle) is much larger than the radius of curvature at the *neck*, where the vesicle actually bends back.

$$\Delta C_m{}^2 \to \frac{\pi(\delta/\rho)^2}{\sqrt{(\delta/\rho)^2 - 1}}\left(\arctan\frac{1}{\sqrt{(\delta/\rho)^2 - 1}} + \frac{\pi}{2}\right) \quad (33)$$

This expression is a function of δ/ρ only and is minimal at $\delta/\rho = 1.59845$, where it takes the value $4\pi + 1.89545$.

Appendix C. A Brief Note on Contact Curvature

In the full variational problem, the meridianal radius of curvature at contact, $1/c^*$, is determined by eq 11 and, in particular, increases smoothly with decreasing colloid radius, $a = -1/c_s$, see the dotted line in Figure 7. In seeming contrast to that, our two-parameter variational approach results in a toroid radius ρ—identical on this level of approximation to the contact radius of curvature—which is a discontinuous function of a (see Figure 7). This is a natural consequence of the restricted variational ansatz. More explicitly, in the full problem, the meridianal curvature changes smoothly from the contact curvature to the smaller curvature of the spherical cap. If this happens monotonically, the *average* curvature of the rim, to be compared to the toroid curvature $1/\rho$ in the restricted variational ansatz, will be smaller than the contact curvature. This can for instance be seen in Figure 10. However, the converse may happen as well. Figure 14 shows an example of a colloid−vesicle complex in the enveloped state determined from the full variational problem (i.e., solving the shape equation[23] under the constraint of fixed volume and area). It can be seen clearly that the vesicle curvature in the rim is now much *larger* than the contact curvature; accordingly, representing this state within the two-parameter model would result in a toroid radius ρ that is *smaller* than the radius of curvature at contact. In brief, because the notions of contact curvature and average curvature at the rim are different in the full variational problem but necessarily equal in the two-parameter ansatz, the rigorous eq 11 applying to the contact curvature does not apply to $1/\rho$.

References and Notes

(1) Lodish, H.; Berk, A.; Zipursky, S. L.; Matsudaira, P.; Baltimore, D.; Darnell, J. *Molecular Cell Biology*, 4th ed.; W. H. Freeman & Company: New York, 2000.

(2) Baker, T. S.; Olson, N. H.; Fuller, S. D. *Microbiol. Mol. Biol. Rev.* **1999**, *63*, 862.

(3) To be more precise, the infection of cells by animal viruses takes place most commonly along the endocytic pathway. (There are some cases in which the virion instead fuses with the membrane.) For plant or fungal cells—although they are eukaryotes—the mechanisms are quite different due to the profoundly different nature of the cell membrane. Moreover, bacterial cells are infected by viruses (called "phages") that almost always inject their genome into the cytoplasm rather than entering as a whole.

(4) Marsh, M., Ed. *Endocytosis*; Frontiers in Molecular Biology 36; Oxford University Press: Oxford, U.K., 2001. van Deurs, B.; Petersen, O. W.; Olsnes, S.; Sandvig, K. *Int. Rev. Cytol.* **1989**, *117*, 131. Bestermann, J. M.; Low, R. B. *Biochem. J.* **1983**, *210*, 1. Silverstein, S. C.; Steinman, R. M.; Cohn, Z. A. *Annu. Rev. Biochem.* **1977**, *46*, 669.

(5) Kielian, M.; Jungerwirth, S. *Mol. Biol. Med.* **1990**, *7*, 17. Marsh, M. *Biochem. J.* **1984**, *218*, 1.

(6) Rhee, S. S.; Hui, H.; Hunter, E. *J. Virol.* **1990**, *64*, 3844.

(7) Garoff, H.; Hewson, R.; Opstelten, D.-J. E. *Microbiol. Mol. Biol. Rev.* **1998**, *62*, 1171.

(8) Dietrich, C.; Angelova, M.; Pouligny, B. J. *Phys. II Fr.* **1997**, *7*, 1651.

(9) Israelachvili, J. N. *Intermolecular and Surface Forces*, 2nd ed.; Academic Press: London, 1998.

(10) Safran, S. A. *Statistical Thermodynamics of Surfaces, Interfaces, and Membranes*; Frontiers in Physics, Vol. 90; Perseus: Cambridge, MA, 1994.

(11) Evans, E.; Needham, D. *J. Phys. Chem.* **1987**, *91*, 4219.

(12) Helfrich, W. *Z. Naturforsch.* **1973**, *28c*, 693.

(13) Strictly speaking, phospholipid bilayers are permeable to water on sufficiently long time scales, so the requirement of volume conservation needs a justification. Dietrich et. al[8] found that the initial adhesion process occurs within a few milliseconds (and it can be expected to proceed even more rapidly for smaller colloids). On such short time scales, permeation of water cannot significantly alter the volume of the vesicle, and it may thus be considered as constant. We will make the same assumption in our own model. One should bear in mind, though, that on longer time scales the increased pressure inside the vesicle can relax, thereby lowering the membrane tension and influencing the degree of wrapping.

(14) As we have mentioned, there is a second source of tension, which originates from the fact that reducing the excess area of a fluctuating membrane also reduces its entropy. See, for instance: David, F.; Leibler, S. J. *Phys. II Fr.* **1991**, *1*, 959. However, we will disregard this contribution in the present work.

(15) A useful approximate conversion is dyn/cm = erg/cm$^2 \approx {}^1/_4 k_BT$/nm^2.

(16) The point of full wrapping is determined by the requirement $\partial(E_{ad} + E_{ten})/\partial z|_{z=2} = 0$. Close to $z = 2$, the constraint of volume conservation can be approximated by $R^3 = R_0{}^3 + a^3$. Inserting the expressions for E_{ad} and E_{ten} into this equation gives the condition

$$\frac{\zeta/2 + \epsilon}{1 - \epsilon} = \tilde{a}^2 - 1 + (1 + \tilde{a}^3)^{2/3} \approx \tilde{a}^2 + \frac{2}{3}\tilde{a}^3$$

The solution of the cubic equation can be written as an expansion in the left-hand side, which gives eq 6. Note that this equation incorporates higher order corrections in a/R_0 compared to the result presented in ref 8.

(17) If at some point the mean curvature is zero but the surface is not flat, the Gaussian curvature is negative, so the local environment is a saddle point. The only contribution to the bending energy then comes from the second term in eq 7, which in this sense measures the energy cost of a saddle-like deformation. Note, however, that it also contributes to the energy at points that are *not* saddle-points.

(18) Do Carmo, M. P. *Differential Geometry of Curves and Surfaces*; Prentice Hall: New Jersey, 1976.

(19) The bending modulus for lipid bilayers is typically in the range of a few tens of k_BT. However, it is rather difficult to measure precisely, and experimentally obtained values for a given lipid may deviate by as much as a factor of 2. See, for instance: Seifert, U.; Lipowsky, R. In *Structure and Dynamics of Membranes*; Lipowsky, R., Sackmann, E., Eds.; Handbook of Biological Physics, Vol. 1A; Elsevier: Amsterdam, 1995.

(20) Seifert, U. *Adv. Phys.* **1997**, *46*, 13.

(21) Landau, L. D.; Lifshitz, E. M. *Theory of Elasticity*, 3rd ed.; Butterworth-Heinemann: Oxford, U.K., 1986; Section 12, problem 6.

(22) Seifert, U.; Lipowsky, R. *Phys. Rev. A* **1990**, *42*, 4768; see eq 2 and footnote 14 therein.

(23) Seifert, U.; Berndl, K.; Lipowsky, R. *Phys. Rev. A* **1991**, *44*, 1182.

(24) Koltover, I.; Rädler, J. O.; Safinya, C. R. *Phys. Rev. Lett.* **1999**, *82*, 1991.

(25) Jülicher, F.; Lipowsky, R. *Phys. Rev. E* **1996**, *53*, 2670.